

HELIOSEISMIC HOLOGRAPHY OF ACTIVE-REGION SUBPHOTOSPHERES

(Invited Review)

D. C. BRAUN^{*,†} and C. LINDSEY

Solar Physics Research Corporation, 4720 Calle Desecada, Tucson, AZ 85718, U.S.A.

(e-mails: dbraun@solar.stanford.edu; lindsey@sprc.com)

(Received 13 October 1999; accepted 3 February 2000)

Abstract. The development of solar acoustic holography has opened a major new diagnostic avenue in local helioseismology. It has revealed ‘acoustic moats’ surrounding sunspots, ‘acoustic glories’ surrounding complex active regions, and ‘acoustic condensations’ suggesting the existence of significant seismic anomalies up to 20 Mm beneath active-region photospheres. Phase-sensitive seismic holography is now yielding high-resolution maps of sound travel-time anomalies caused by magnetic forces in the immediate subphotosphere, apparent thermal enhancements in acoustic moats, and Doppler signatures of subsurface flows. It has given us the first seismic images of a solar flare, and has uncovered a remarkable anomaly in the statistical distribution of seismic emission from acoustic glories. Seismic holography will probably give us the means for early detection of large active regions on the far-surface of the Sun, and possibly of deep subsurface activity as well. This powerful diagnostic now promises a new insight into the hydromechanical and thermal environments of the solar interior in the local perspective.

1. Introduction

Over the past three years the application of solar acoustic holography to observations from the Michelson Doppler Imager (MDI) aboard the Solar Heliospheric Observatory (SOHO) spacecraft has opened local helioseismology to a windfall of new discoveries. It has revealed ‘acoustic moats’ surrounding sunspots, ‘acoustic glories’ surrounding complex active regions, ‘acoustic condensations’ suggesting the existence of remarkable seismic anomalies 10–20 Mm beneath active-region photospheres, and has given us the first phase-coherent images of a solar flare. These discoveries are all results of the application of a diagnostic which we have been performing on electromagnetic radiation with our eyes for eons: simple phase-coherent imaging.

Helioseismic holography is quite literally the phase-coherent computational reconstruction of the acoustic field into the solar interior based on seismic disturbances observed on the near surface, so as to render stigmatic images of subsurface

*Visitor, Joint Institute for Laboratory Astrophysics, University of Colorado, Boulder, CO 80309-0440, U.S.A.

† Current mailing address: Colorado Research Associates, 3380 Mitchell Lane, Boulder, CO 80301, U.S.A.



sources that have given rise to these disturbances. The practical application of the diagnostic is described in technical detail by Lindsey and Braun (2000). The analyst applies the seismic disturbance observed over the solar surface to drive a model of the solar acoustic medium *in time reverse*. Computationally, the task is to propagate the acoustic disturbances resulting from such a time-reverse application backwards into the interior of the model and sample the acoustic field in ‘focal planes’ at depths of interest. Such a sampling will render an acoustic source in the focal plane by a compact, positive image. An acoustic sink in the focal plane against a background of ambient acoustic noise will likewise be presented sharply in silhouette. If the ‘focal plane’ on which the acoustic model is sampled is moved substantially above or below the depth of the source or sink, the image will simply defocus (see Figure 3 of Lindsey and Braun, 2000). This dependence of the image focus on location of the focal plane lends a powerful depth diagnostic that is familiar to practitioners of optical microscopy or standard optical holography.

Lindsey *et al.* (1996) emphasize the analogy between seismic holography and the function of standard lens optics in the electromagnetic domain. Like electromagnetic holography and lens optics, seismic holography is a formalism in *wave mechanics* and contains a full account for the effects of diffraction. As such, seismic holography is subject to the same fundamental limitations in terms of diffraction and statistics as any other diagnostic based on helioseismic observations. It is likewise open to the full range of optical techniques that have been developed to optimize the informational content of coherent electromagnetic radiation.

Holographic regressions are conveniently expressed in terms of a computational diagnostic which Lindsey and Braun (1997) call the ‘acoustic egression’. For the following discussion, we will use the notation (\mathbf{r}, z) to locate a point at depth z directly beneath a surface position represented by \mathbf{r} . The acoustic egression, $H_+(\mathbf{r}, z, \nu)$, then, is a coherent assessment of the local acoustic disturbance at frequency ν that emanates from the ‘focal point,’ (\mathbf{r}, z) , of the computation based on its succeeding emergence at the overlying solar surface, which is represented at surface location \mathbf{r}' by the complex acoustic amplitude $\psi(\mathbf{r}', \nu)$. In this ‘space-frequency’ context, the egression is represented by an integral of the form

$$H_+(\mathbf{r}, z, \nu) = \int_{a < |\mathbf{r} - \mathbf{r}'| < b} d^2\mathbf{r}' G_+(|\mathbf{r} - \mathbf{r}'|, z, \nu) \psi(\mathbf{r}', \nu) \quad (1)$$

(see Equation (5) of Lindsey and Braun, 2000). Here G_+ is a Green’s function that expresses how a monochromatic point disturbance at $(\mathbf{r}', 0)$ propagates backwards in time to (\mathbf{r}, z) , or equivalently, forward in time from (\mathbf{r}, z) to $(\mathbf{r}', 0)$. The ‘acoustic ingression,’ H_- , is the time reverse of the egression H_+ . It rather expresses waves coherently converging *into* the focal point, (\mathbf{r}, z) to contribute *to* the local disturbance, rather than emerging *from* it. The ingression is computed simply by replacing the Green’s function, G_+ , in Equation (1) by its complex conjugate, G_- . The computational regressions are performed over an annular region, the ‘pupil,’

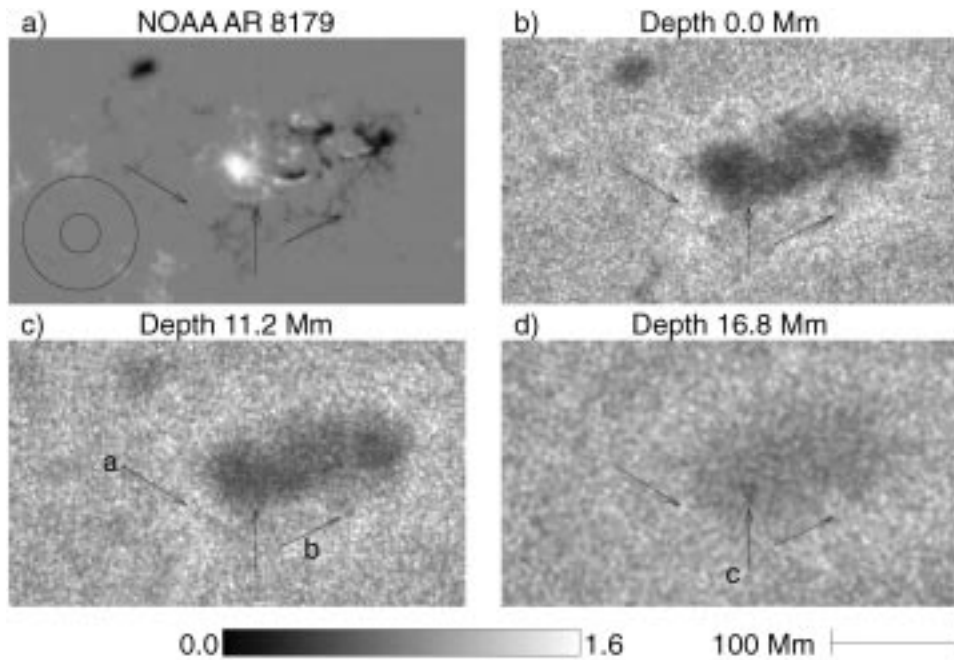


Figure 1. Helioseismic images of NOAA AR 8179 obtained for the 24 hr period 16 March 1998 over a range of depths. Frame (a) shows a concurrent SOHO SOI-MDI magnetogram. (b), (c), and (d) show 5-mHz helioseismic images of the regions at depths 0, 11.2 and 16.8 Mm, respectively. Arrows labeled 'a' and 'b' in (c), and 'c' in (d) indicate condensations that appear in those frames. The arrows are copied in all four frames at the same positions. The linear grey scale at the bottom applies to all of the helioseismic images which are normalized to unity for the mean quiet Sun. The pupil for the egression computations is represented by the annular template at the lower left of Frame (a).

with inner radius a and outer radius b centered at \mathbf{r} , the surface location directly overlying the focal point, (\mathbf{r}, z) .

2. Depth Diagnostics

Lindsey and Braun (1990, 1997) elaborated on the utility of using focus-defocus as a depth diagnostic. Illustrations based on computational regressions of artificial seismic noise are presented by Lindsey and Braun (1997), and by Figures 3 and 5 of Lindsey and Braun (2000). Braun and Lindsey (1999) find that the higher acoustic frequencies, with their finer spatial resolution, offer depth diagnostics far superior to those obtained from frequencies near 3 mHz, even though the latter are known to represent a far greater acoustic power.

Figure 1, taken from Braun and Lindsey (1999), illustrates single-skip seismic holography of NOAA AR 8179 in 5 mHz acoustic radiation employing observations from the SOHO-MDI. Frame (a) shows an MDI magnetogram of the region. The pupil for these computations is an annulus with inner radius $a = 15$ Mm

and outer radius $b = 45$ Mm (see annular template at lower left of Figure 1(a)). Figures 1(b–d) show egression power maps integrated over a 24 hr period at depths ranging from 0 to 16.8 Mm. Quite conspicuous in Figure 1(b) is a general deficit of acoustic egression power inside the magnetic region and a halo of excess 5 mHz emission largely surrounding the entire active region complex. The latter feature is called the ‘acoustic glory’ and is discussed further in Section 3.2. The arrows labeled ‘a’, ‘b’, and ‘c’ point to conspicuous ‘acoustic condensations’ that congeal in focal planes at the depths at which the arrows are labeled. As in the simulation shown in Figure 3 of Lindsey and Braun (2000), the granular texture of the background represents statistical fluctuations, not significant spatial variations in the quiet-Sun egression power.

It is important to keep in mind that as the focal plane submerges (Figures 1(c) and 1(d)) the sharp signature of the magnetic region at the surface, rather than disappearing, simply defocuses. The diffuse signature that extends beneath the active region, to the deepest focal planes, is called the ‘acoustic stalactite’. This is an expected artifact of an acoustic absorber at any level, however narrow in depth, and must not be mistaken for real acoustic absorption extending substantially beneath the surface. Careful modelling is generally required to discriminate between submerged acoustic anomalies and the acoustic stalactites of superficial ones. Examples are presented in Section 2 (see Figure 3) and Section 5 (see Figure 5) of Lindsey and Braun (2000). In well appropriated egression computations, acoustic silhouettes of superficial acoustic anomalies invariably defocus rapidly as the focal plane submerges. The suggestion that the condensations represent actual submerged perturbations is based on signatures that become more compact as the focal plane submerges, attaining their optimum sharpness substantially beneath the surface.

While acoustic condensations encountered to date have often appeared near sunspots, (e.g., that indicated by Arrow c in Figure 1(d)), they do not generally lie directly beneath sunspots, and can appear tens of Mm from any sunspot. Based on considerations discussed by Lindsey *et al.* (1996), it is difficult to understand the condensations in terms of a direct signature of magnetic flux tubes. Magnetic pressures typical of sunspots are dwarfed by gas pressure at great depths, and it is therefore difficult to see how the Lorentz forces alone could manifest the acoustic modulus needed to significantly scatter or absorb acoustic radiation more than 10 Mm beneath the photosphere. Lindsey and Braun (1998a) and Braun and Lindsey (1999) propose that the condensations are the signatures of thermal or Doppler perturbations. However, other interpretations need to be considered, including the possibility that the condensations could accidentally result from phase errors introduced by surface magnetic regions in the pupil of the computation.

The egression power image at zero depth in Figure 1 should not be confused with a simple acoustic power map of the local wave amplitude as directly observed. Each pixel in Figure 1(b) is a coherent representation of waves that have traveled thousands of km from the pixel, and deep beneath the solar surface, to re-emerge

into the pupil thousands of km away from the source. These computations show the solar surface from a ‘subjacent vantage,’ the perspective of a submerged acoustic observer looking upward, into the bottom of the active region from beneath it (see Section 4 of Lindsey and Braun, 2000).

Apart from the acoustic condensations, most of the features in Figures 1(b–d), including both the general magnetic-associated deficit and the surrounding acoustic glory, seem to be superficial. Braun *et al.* (1998) and Lindsey and Braun (1998b) find that 3 mHz egression power deficits in sunspots are consistent with absorption that occurs predominantly within a few Mm or less of the photosphere. This is in qualitative agreement with models that attribute acoustic absorption by magnetic regions to the coupling of compression waves with slow magneto-acoustic modes by a spreading magnetic field at or just beneath the active-region surface (Cally, 2000). It is also consistent with the sharp decrease in the acoustic deficit measured by Hankel analysis (Braun, Duvall, and LaBonte, 1988) for low- ℓ waves emerging from sunspots. Fan, Braun, and Chou (1995) carefully modelled sunspots in terms of superficial acoustic perturbations, successfully reproducing the results of Hankel analysis. Braun *et al.* (1998) point out that low- ℓ waves have a large skip distance, and that these therefore tend to avoid absorption simply by skipping beneath the magnetic surface, where the absorption occurs. To be quite general, it is in the near solar interior, just beneath the photosphere, that seismic holography encounters by far the strongest signatures. Indeed, helioseismic holography has revealed some striking new phenomena here that have eluded all other techniques. We discuss the primary results of these applications in the following section.

3. Scientific Results from Seismic Holography

The discovery that sunspots and solar active regions are strong absorbers of incident acoustic (p -mode) radiation (Braun, Duvall, and LaBonte, 1988) provided a major impetus for the recognition of ‘local helioseismology’ as a major emerging field of solar research, and its cogent promotion by Braun *et al.* (1992) and subsequent publications. The concept of phase-coherent helioseismic imaging was introduced, discussed and developed by Lindsey and Braun (1990), Braun *et al.* (1992), Lindsey *et al.* (1996), and Lindsey and Braun (1997) to probe the three-dimensional distribution of local acoustic anomalies beneath the solar photosphere. The first application of seismic holography, to observations from the Taiwan Oscillations Network (Chang *et al.*, 1997), confirmed the well-known acoustic absorption by sunspots, discovered by Braun, Duvall, and LaBonte (1988) using Hankel analysis. A remarkable array of new discoveries proceeded from the application of the technique to SOHO-MDI observations, including the resolution of a number of persistent puzzles that had been posed by previous diagnostics. In general, the scientific results obtained from holographic imaging are in excellent agreement with

those obtained from Hankel analysis. These include the absorption and phase-shifts of p modes propagating through active regions.

3.1. THE ACOUSTIC MOAT

The first major discovery from seismic holography was that of the ‘acoustic moat,’ a region showing a general deficit of 10–30% in 3–4 mHz acoustic emission which extends *far beyond* the sunspot over distances of 30–60 Mm (Braun *et al.*, 1998). The acoustic moat correlates to some degree with surrounding plage, but tends to be more contiguous and often extends into regions that are magnetically quiet. It is now evident that all substantial sunspots develop acoustic moats within hours of their appearance at the photosphere. Examples are shown in Figure 2. The left column in the Figure shows magnetograms of regions whose respective 1–4-skip egression power maps are shown in the right column. The egression power maps were integrated over periods of 72 hr in 3 mHz radiation. The sunspots in all of these images are rendered by strong, compact acoustic deficits coincident with their photospheric locations. The acoustic moats appear as extended, weaker, and sometimes somewhat diffuse acoustic deficits surrounding the sunspot and often encompassing nearby plages.

Isolated plages themselves generally render a substantial acoustic deficit, a well-known result of Hankel analysis (Braun, 1995). However, acoustic moats generally encompass regions free of surface magnetic fields, and therefore plages. A clear example is seen in Figure 2(d), in the corridor bounded by the dashed vertical lines. The line-of-sight magnetic field in this corridor is plotted in Figure 3(a) above a plot of the egression power (b). This shows the acoustic power deficit representing the acoustic moat extending some 60 Mm into the non-magnetic quiet Sun in both directions. Egression-power maps of simulated noise similar to those shown in Figure 3 of Lindsey and Braun (2000) apprise us that the egression power signature of a compact absorber would have a faint surrounding halo primarily due to acoustic diffraction effects, but with only a fraction of the egression power deficit exhibited by the acoustic moat. Integrated over its the entire area, the acoustic moat generally accounts for the major fraction of the active-region acoustic deficit.

While the acoustic moat may have its own absorption mechanism, it is possible that it simply scatters, by means of associated Doppler or thermal perturbations, the acoustic deficit introduced by the nearby sunspot photosphere. Braun *et al.* (1998) and Lindsey and Braun (1998a) proposed that the acoustic moat signifies an anomalous convection cell flowing rapidly outward not far beneath the solar surface. Such a convection cell would be driven by heat accumulation caused by the blockage of convective transport through the sunspot photosphere (Meyer *et al.*, 1974; Nye, Bruning, and LaBonte, 1988; Fox, Sophia, and Chan, 1991). Braun and Lindsey (2000) propose that the dynamics of such a convection cell must be such as to spread the heat blocked by the sunspot into a layer sufficiently thin that the thermal excess due to the blockage reaches the surface efficiently through normal

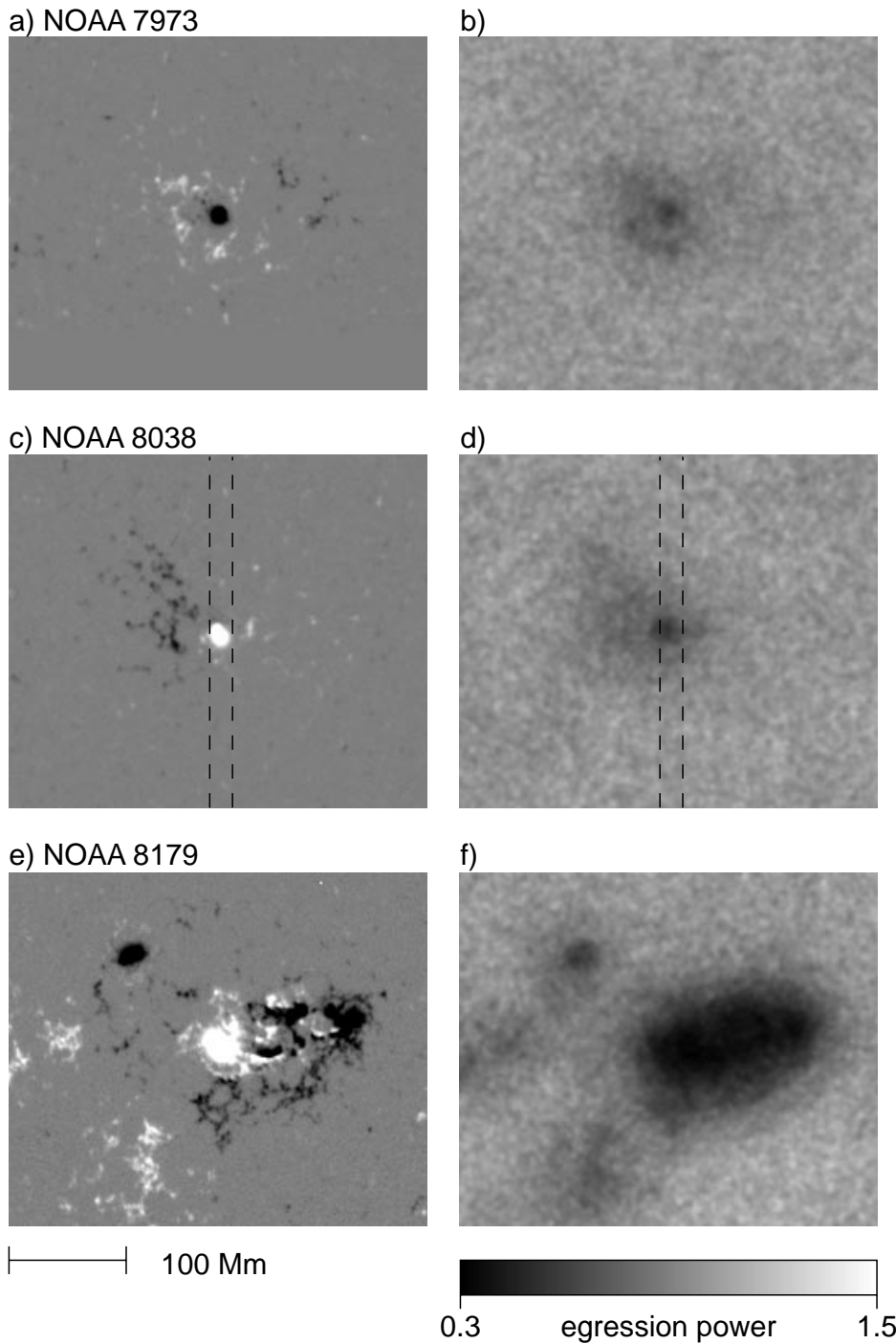


Figure 2. Acoustic moats of isolated sunspots and a complex active region. The top row, Frames (a) and (b), shows a SOHO-MDI magnetogram and an egression power map, respectively, of NOAA active regions 7973 on 25 June 1996. The middle row, (c) and (d), shows the same for 8038 on 11 May 1997. The bottom row, (e) and (f), likewise shows 8179 on 16 March 1998. The egression power maps are integrated in a 1 mHz passband centered at 3 mHz, each integrated over a 72 hr period at depth zero. The vertical dashed lines in the middle row indicate a corridor across which the line-of-sight magnetic-field, B , and egression-power, $|H_+|^2$, are integrated and plotted in Figure 3.

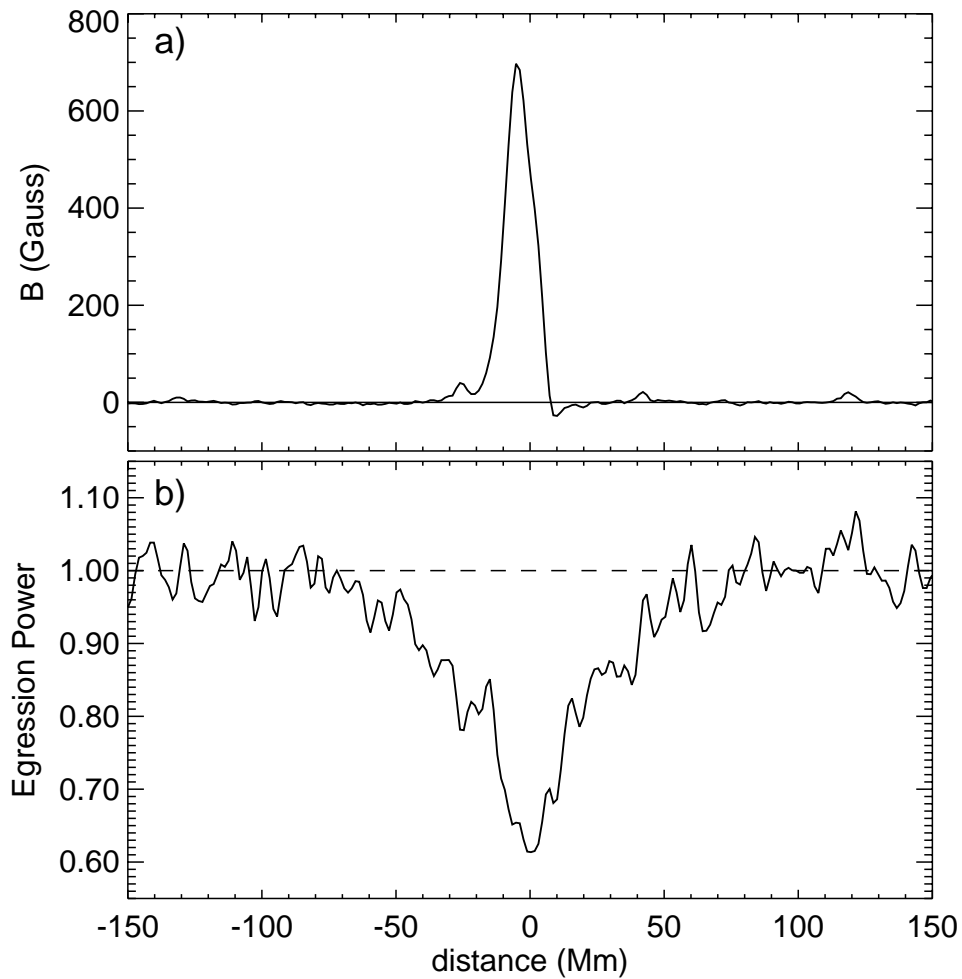


Figure 3. Plots of line-of-sight magnetic field, B (a) and egression power, $|H_+|^2$ (b) of NOAA 8038 as a function of distance north of sunspot center, integrated over the width of the corridor shown by vertical dashed lines in (c) and (d) of Figure 2.

supergranular transport. This would explain the remarkable horizontal extent of the acoustic moat and the general lack of a conspicuous excess in photospheric luminosity in the immediate periphery of the sunspot (Parker, 1974; Rast *et al.*, 1999). It also suggests that the horizontal extent of the moat would be a fairly direct function of the area occupied by the sunspot. Figure 4 shows the acoustic moat of a decaying sunspot, apparently rapidly collapsing.

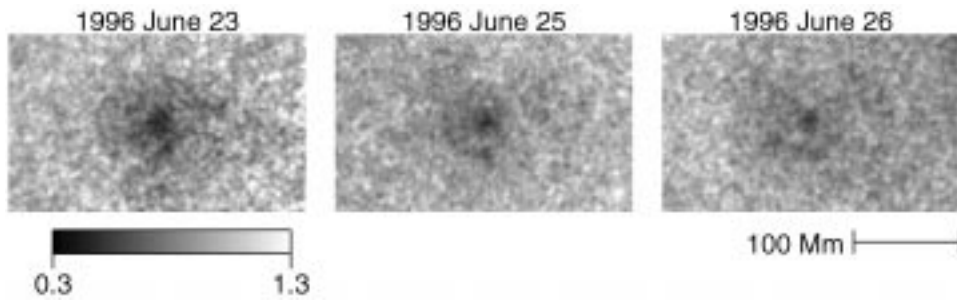


Figure 4. Evolution of the acoustic moat surrounding the sunspot in NOAA AR 7973 from 23 June 1996 (left) to 26 June (right). The egression power maps are each integrated at depth zero over the 2.5–3.5 mHz frequency band for a 24 hr period.

3.2. ACOUSTIC GLORIES

Another remarkable discovery from holography was that of the ‘acoustic glory,’ a prominent halo of excess 5–6 mHz seismic emission around some active regions, particularly growing multipolar magnetic regions (Braun and Lindsey, 1999). A conspicuous example is seen in Figure 1(b). At 5 mHz the acoustic glories often contain small, point-like seismic emitters that average 1.5 times the acoustic power of the quiet Sun. These tend to congeal in strings. Donea, Lindsey, and Braun (2000) show that the small emitters that characterize acoustic glories at 5 mHz are nearly all confined to the quiet Sun, usually bordering weak magnetic regions and sometimes marking neutral lines separating positive and negative polarity. The individual emitters which they examined tended to sustain a continuous acoustic excess, remaining stationary for periods of 10–20 hr as the outer boundary of the active region expanded towards it.

Figure 5 secures that the acoustic glory is not an artifact of phase errors or other acoustic perturbations which the active region introduces into the pupil directly. The test here was to compute the egression power with the major surface magnetic regions masked out. The result is an image which is substantially degraded by diffraction in regions where the mask vignettes the pupil. The acoustic glory nevertheless remains clearly apparent around most of the periphery of the region.

Donea, Lindsey, and Braun (2000) find that the stronger emitters comprising acoustic glories show a distribution in egression power that significantly saturates at values 4–6 times the quiet-Sun average by comparison to the quiet Sun. The distribution of power emanating from the quiet Sun itself accurately conforms to the exponential distribution equivalent to standard Gaussian noise. The saturation of high-frequency emission from the acoustic glories may help us to understand the mechanism of acoustic emission at all frequencies, including both the nominal emission from the quiet Sun and the excess that characterizes the acoustic glories themselves. This may be the signature of acoustic non-linearities related to even-

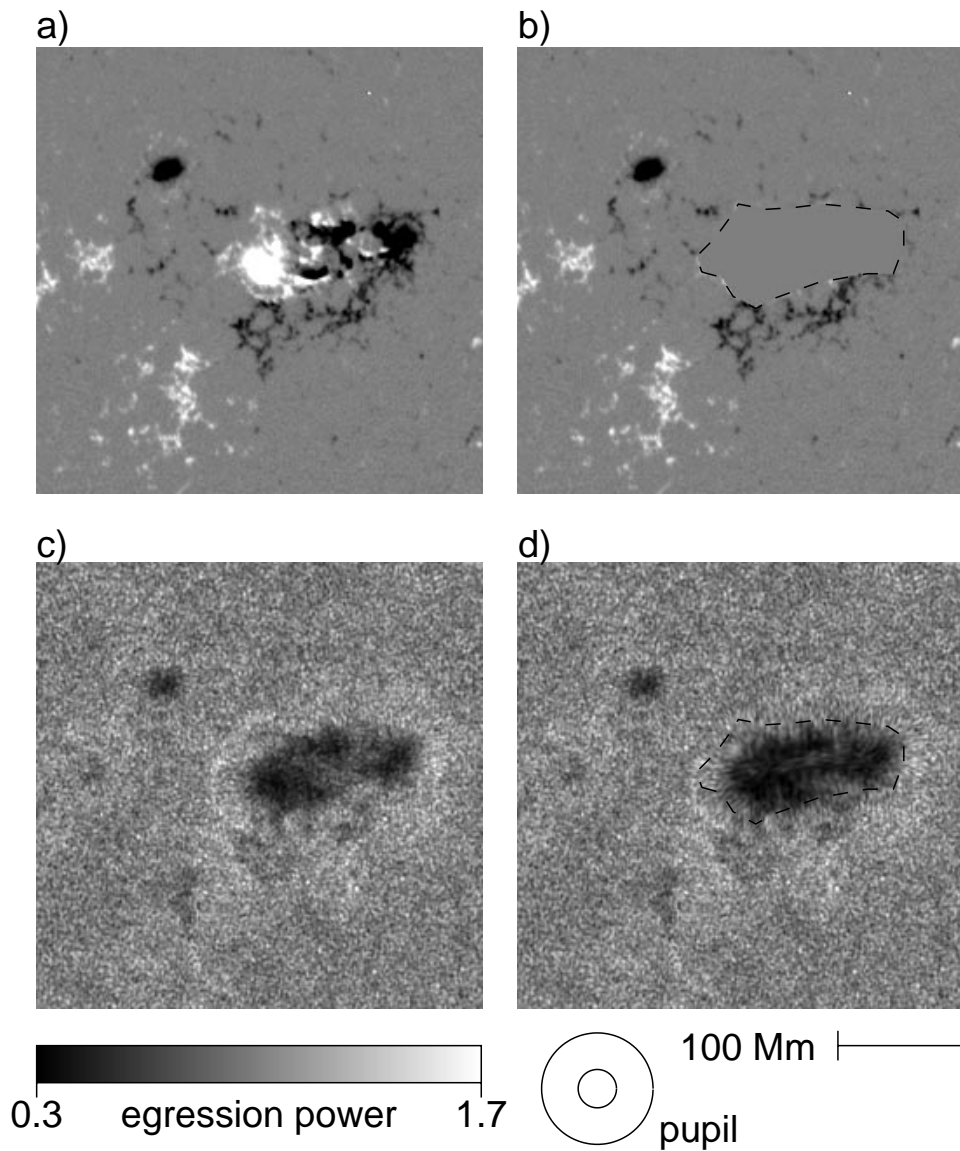


Figure 5. An experiment with masks. Egression power maps of NOAA AR 8179 at depth zero are computed normally in (c), shown beneath a cospatial magnetogram (a). In (d) the egression power is plotted with the acoustic field, ψ , omitted (set to zero) in the region enclosed by the dashed curved shown in Frames b and d. The acoustic glory near the mask is significantly smeared by diffraction in the direction perpendicular to the mask boundary. However, it is still clearly apparent in (d) in most places where it appears in (c). The size of the pupil used in the egression computations is indicated below (d).

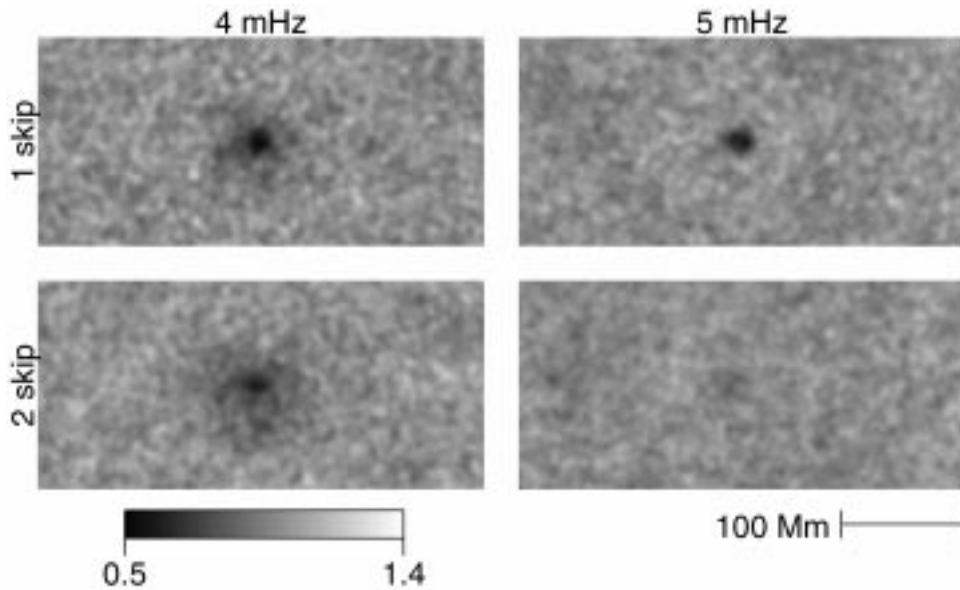


Figure 6. Single skip (*upper row*) and double-skip (*lower*) egression power maps of NOAA AR 7973 (25 June 1996) at depth zero are computed in 1 mHz passbands centered at 4 mHz (*left column*) and 5 mHz (*right*). These images are smeared to approximately 15 Mm to enhance the acoustic moat.

tual limits in the general mechanism that supplies the free energy that drives the acoustic emission.

Single isolated sunspots show only a weak, diffuse excess in egression power surrounding them (Lindsey and Braun, 1999). However, this explains the apparent decrease in the acoustic absorption coefficient at 5 mHz inferred from Hankel analysis (Braun, 1995). The disproportionate strength of the acoustic glory surrounding the large active region in Figure 5 is conspicuous when compared with its nearly invisible counterpart around the isolated sunspot to its upper left. This characteristic distinguishes this new phenomenon from the well-known ‘acoustic halos’ that appear in plain Doppler acoustic power maps of the solar surface at 6 mHz. These surround *all* magnetic features, including isolated sunspots (see Braun *et al.*, 1992; Brown *et al.*, 1992; Hindman and Brown, 1998). Figure 4 of Donea, Lindsey, and Braun (2000), in this volume, shows comparative images of acoustic power halos and acoustic glories. These features are indicative of substantially enhanced *surface motion* but generally *not* enhanced wave emission.

3.3. THE SPECULAR QUALITY OF THE QUIET PHOTOSPHERE

Multiple-skip holography (see Section 8.1 of Lindsey and Braun, 2000) offers us an assessment of the specular quality of the photosphere as a reflector. Figure 6, taken from Lindsey and Braun (1999) demonstrates the strong dependence of photospheric reflectivity on acoustic frequency by comparing 1- and 2-skip egression

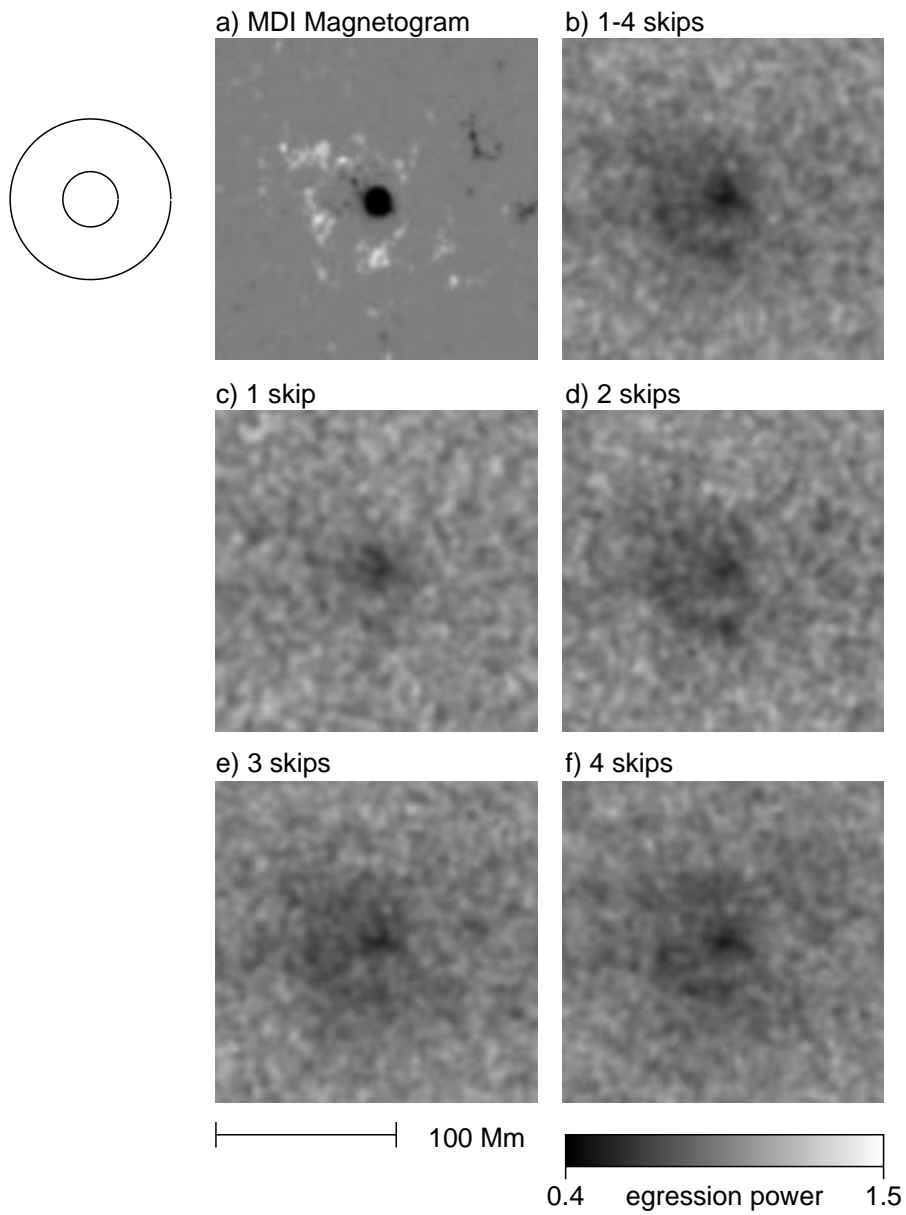


Figure 7. Multiple-skip holography of 3 mHz acoustic radiation. Frame (a) shows an MDI magnetogram of the region, for reference. (c)–(f) show 24 hr egression-power maps of NOAA AR 7973 computed in a 1 mHz bandpass centered at 3 mHz for disturbances that have completed 1, 2, 3, and 4 skips, respectively, from the focal point (depth zero). Frame (b) shows the acoustic power computed from the four egression amplitudes coherently superposed. The annulus at upper left represents the pupil of the egression computations.

power images of a sunspot. Figures 1(a) and 1(b) show 1-skip images of the sunspot in 4 mHz acoustic radiation. Figures 1(c) and (d) show 2-skip images of the same. The 2-skip images depend on a single reflection of the acoustic radiation from the source back into the solar interior before it arrives at the pupil. That signatures of both sunspot and acoustic moat remain sharp and clean in the 4 mHz 2-skip image depends on the photosphere being a high-quality specular reflector that preserves the coherence of the incident waves. The abrupt disappearance of both sunspot and acoustic moat in 2-skip images for frequencies above ~ 4.5 mHz confirm findings by Duvall *et al.* (1993), based on time-distance correlations, that the photosphere is a poor specular reflector above its acoustic cutoff frequency.

Given that 5 mHz waves substantially penetrate upward into the photosphere, where radiative damping is strong, this result might have been somewhat anticipated. However, the mechanism could be more complicated than just a matter of damping. It should be kept in mind that the photosphere might very well promptly return a substantial fraction of the acoustic radiation it receives after simply destroying its phase coherence.

For 3 mHz acoustic radiation, the specular quality of the photosphere appears to be quite high. Figure 7 shows egression-power images of a sunspot for up to four skips (Figures 7(c)–(f)). Also shown is the power of a coherent sum of the four egression amplitudes (Figure 7(b)). The sunspot and acoustic moat remain clearly visible in acoustic disturbances that are completing their fourth skip. The contrast of the 2-skip egression-power map appears to be significantly greater than that of the 1-skip map. The lower contrast in the 1-skip map may be a result of acoustic errors introduced by plages, which occupy a significant part of the 1-skip pupil. Comparisons between different n -skip egression-power maps show a substantial correlation in statistical variations of their backgrounds. The result is that the coherent sum of the n -skip egression amplitudes accomplishes only a limited improvement of the sunspot and acoustic moat signatures with respect to statistical noise.

3.4. SEISMIC IMAGES OF A SOLAR FLARE

Kosovichev and Zharkova (1998) discovered a significant acoustic signature in the SOHO-MDI observations emanating from NOAA AR 7978 in the 1-hr period following the large solar flare of 9 July 1996. Figure 8 shows chromatic images of this signature, taken from Donea, Braun, and Lindsey (1999). The Figure shows egression power images in 2 mHz bands centered at 3.5 mHz (left column) and 6.0 mHz (right). The top frames show the egression power in the respective bands integrated over a 2-hr interval encompassing the flare. The underlying frames show the instantaneous egression power at the times indicated. These render an acoustic source that is significantly extended, some 18 Mm in the north-south direction. The 6 mHz egression, remarkably, emerges at full acoustic intensity some 3.5 min after the 3.5 mHz. The 6 mHz signature is actually much *weaker* than the latter, in terms

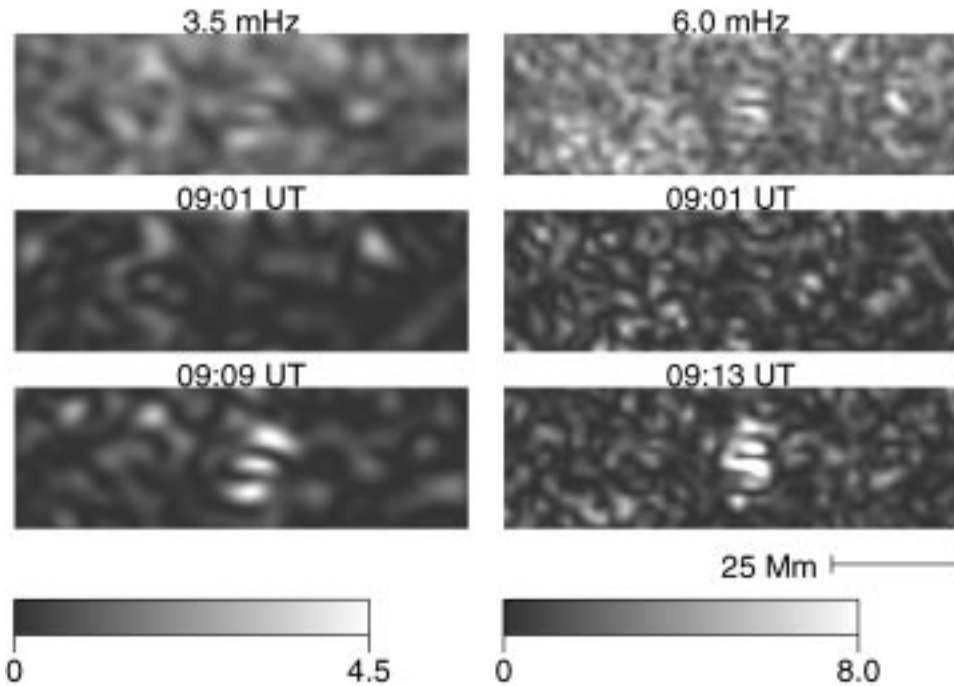


Figure 8. Instantaneous 1-skip egression-power images of the solar flare of 9 July 1996 in NOAA AR 7978 in 2-mHz bands centered at 3.5 mHz (*left*) and 6 mHz (*right*), taken from Donea, Braun and Lindsey (1999). The onset of the flare in X-rays was approximately 09:07 UT.

of absolute power. However, it is significantly stronger compared to the ambient noise at the higher frequencies.

3.5. PHASE SENSITIVE HOLOGRAPHY

In addition to their distinctive absorption and emission properties, sunspots, plages, and acoustic moats invariably produce significant *phase shifts* in acoustic radiation that encounters them, consistent with variations in sound-travel times that result from thermal and Doppler perturbations. Lindsey and Braun (1997) introduced phase sensitive holography to image such phase shifts. This is accomplished by phase correlating the egression and the ingression (see Section 7 of Lindsey and Braun, 2000) to render statistics entirely analogous to the time-distance correlations of Duvall *et al.* (1996), and in particular to what Braun (1997) calls ‘annulus-annulus correlations’. At 3–4 mHz a uniformly strong correlation between the ingression and egression is observed over the quiet Sun, because it reflects the ingressing spectrum specularly, preserving the horizontal wavenumber, ℓ , of the mode. Acoustic perturbations at the surface generally cause a local shift in the phase of the correlation. A relatively stochastic perturbation may impair coherence and thereby reduce the amplitude of the correlation.

The first application of phase-sensitive holography, to observations from the Taiwan Oscillations Network (Chen *et al.*, 1998), confirmed the well-known acoustic scattering phase-shifts of sunspots, determined by Hankel analysis (Braun, 1995) and subsequently confirmed by time-distance correlation measurements (Duvall *et al.*, 1996; Braun, 1997). Applications of holographic phase diagnostics to SOHO-MDI observations now clearly show significant travel-time reductions for isolated plages and acoustic moats as well as sunspots.

Figure 1 of Braun and Lindsey (2000) shows a map of the egression-ingression phase-shift of NOAA AR 8179. Unlike the egression power signature, the sound travel-time anomalies, determined from the phases, correlate sharply with surface magnetic regions. Sunspots are characterized by one-way travel-time reductions of order 40 s. Isolated plages render travel-time reductions up to 15 s. Braun and Lindsey (2000) interpret these reduced travel times in terms of an ‘acoustic Wilson depression’ approximately in logarithmic proportion to magnetic pressure that applies to all surface magnetic fields in excess of approximately 10 G. A comparison of sound travel times for magnetic regions in acoustic moats with those of isolated plages clearly shows that the acoustic moats have additional time delays of order 3–5 s. This might be explained by the thermal excess, caused by heat blockage, which would drive the moat flow (see discussion in Section 3.1). Braun and Lindsey (2000) present statistics to suggest that the entirety of the frequency shifts of global modes with the solar cycle (Jiménez-Reyes *et al.*, 1998) can be explained by phase shifts due to plages, acoustic moats, and sunspots, in that order of importance.

It should be understood that perturbations which simply refract or scatter isotropic acoustic radiation entirely depend on phase correlations for their detection. Simple acoustic-power holography readily reveals acoustic sources and sinks. However, under isotropic illumination, pure scatterers simply replace radiation which they block with scattered radiation from some other direction. This renders them invisible to simple acoustic power holography for lack of contrast against the illuminating background. Because strong absorbers create an anisotropy in the local acoustic field, scatterers near strongly absorbing active-region photospheres may render a significant egression-power signature. However, in an acoustically isotropic environment, the detection of a pure scatterer requires phase-correlation diagnostics.

3.6. COHERENT REFLECTIVITY OF ACTIVE-REGION SUBPHOTOSPHERES

Phase-sensitive holography of the quiet Sun at the higher frequencies confirms the conclusion of Duvall *et al.* (1993) that the quiet photosphere absorbs, or otherwise incoherently scatters, acoustic radiation at frequencies above ~ 5 mHz. In the 6 mHz acoustic spectrum, the correlation between the quiet-Sun egression and ingression is undetectable. Surprisingly, this does not apply to active regions. That active regions coherently reflect 6 mHz acoustic noise is demonstrated by Figure 4 of Braun and Lindsey (2000), which maps the phase of the correlation between

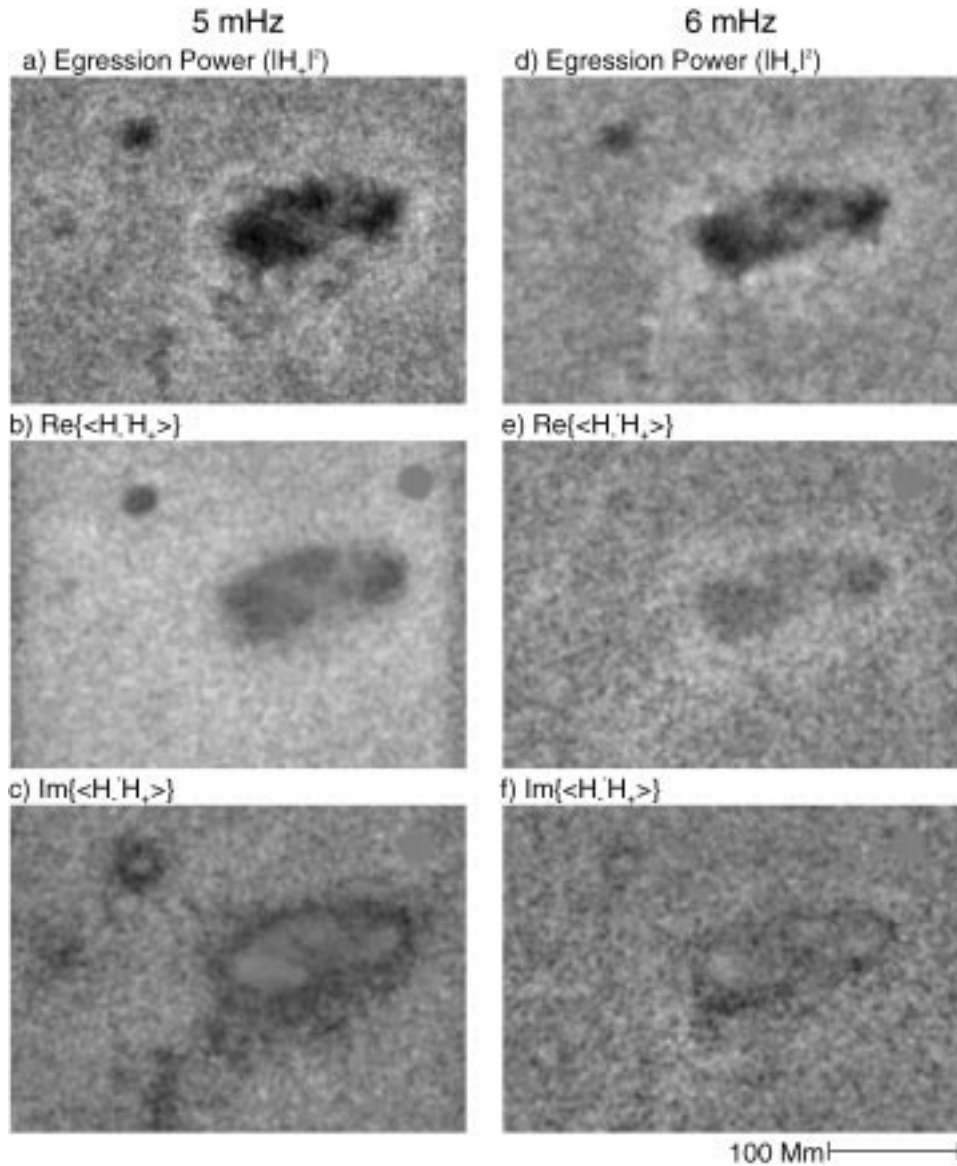


Figure 9. Phase correlation maps between ingression and egression in the 4.5–5.5 mHz band (*left*) and 5.5–6.5 mHz (*right*). The top row (Frames (a) and (d)) show egression power, $|H_+|^2$. The middle and bottom rows show respectively the real and imaginary parts of the phase correlation, $\langle H_-^* H_+ \rangle$, between incoming and outgoing acoustic radiation. The 6-mHz correlation, $\langle H_-^* H_+ \rangle$, is essentially zero in the quiet Sun. Grey dots at upper right of (b), (c), (e), and (f) indicate the grey tone level of zero correlation. This shows that the quiet solar photosphere effectively ingests incoming acoustic radiation and replaces it with locally generated radiation whose phase is uncorrelated. However, the active region shows a correlation that is quite remarkable. The peripheries of active regions are substantial reflectors.

egression and ingression as frequency proceeds from 3 to 6 mHz. Figure 9 illustrates the same, mapping the individual real and imaginary parts of the 5-mHz (left column) and 6-mHz (right column) phase correlations. This remarkable phenomenon may help us to understand what is distinctive about the quiet photosphere such that it so efficiently absorbs upcoming acoustic noise or otherwise destroys its coherence.

4. Future Directions

4.1. DOPPLER DIAGNOSTICS

Lindsey and Braun (2000) describe an extension of the phase diagnostics applied by Braun and Lindsey (2000) which are sensitive to horizontal flows. Figure 10 shows the horizontal Doppler signature of a sample of quiet Sun (Figure 6(a)) and a sunspot (Figure 6(b), NOAA AR 8243) computed by this method. These signatures are as yet uncalibrated. However, applied to the quiet Sun (Figure 6(a)), they clearly show the supergranulation. A conspicuous outflow surrounding the sunspot appears in Figure 6(b). This coincides with the extension of the acoustic moat that appears in egression power (not shown here). An independent, more compact outflow pours from a small, but rapidly developing, sunspot on the north-east periphery of the major outflow from frame center. Outflows surrounding sunspots are already the subject of a large volume of literature based on magnetic tracers and surface Doppler measurements (e.g., Sheeley, 1969; Harvey and Harvey, 1973; Brickhouse and LaBonte, 1988). It now appears that the extended, non-plage-like signature of the acoustic moat in simple egression power could be predominantly the result of Doppler scattering of an acoustic deficit that originates in magnetic photospheres by a rapid underlying upflow and resulting near-subsurface outflow.

4.2. PHYSICS OF p -MODE ABSORPTION BY MAGNETIC REGIONS

Cally and Bogdan (1997) propose that p -mode absorption by magnetic regions is a result of surface coupling of p modes to slow Alfvén modes, which are efficiently dissipated at great depths where the Alfvén speed becomes very small. More recent theoretical work (Cally, 2000) suggests that non-vertical magnetic fields are critical for the efficient coupling of the low- ℓ p modes (whose motion in non-magnetic regions is predominantly vertical) to the Alfvén modes. This suggests that the peripheries of sunspots should show a significantly stronger low- ℓ egression deficit than the centers, where the field tends to be vertical. A careful study including plages and incorporating comparisons with vector magnetograph observations could shed considerable light on the long-standing problem of how magnetic regions contrive to dispose of much of the acoustic power that comes their way.

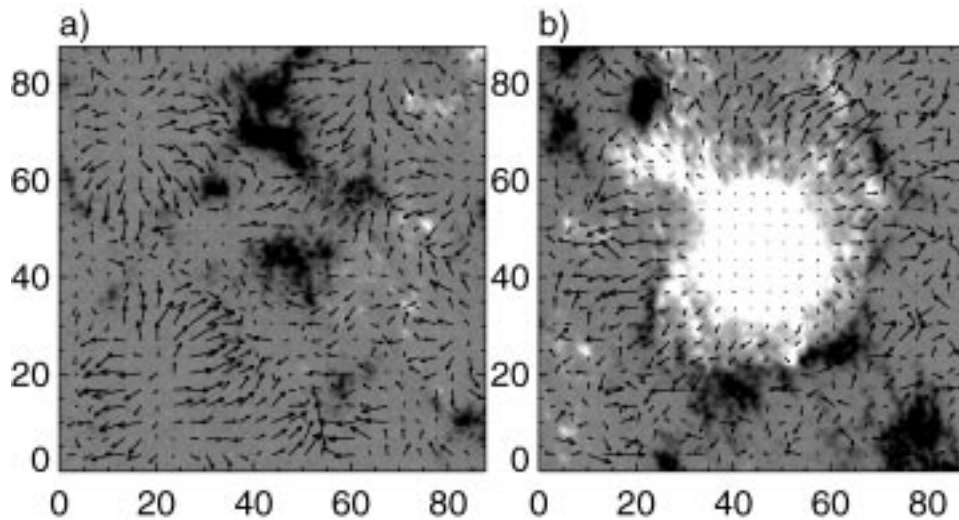


Figure 10. Horizontal Doppler holography applied to high-resolution SOHO-MDI observations of NOAA AR 8243 and its surroundings. (a) shows horizontal flows associated with the supergranulation. (b) shows outflows surrounding a sunspot.

4.3. EMERGING MAGNETIC FLUX

How seismic diagnostics may allow us to substantially anticipate the emergence of completely submerged magnetic flux is not presently clear. Rough estimates by Fan (1999, private communication) of Doppler phase shifts of rising flux tubes are discouraging when these are substantially beneath the solar surface, given dimensions and velocities consistent with her hydrodynamic models. Nevertheless, seismic holography could open any number of new avenues along which to explore forecasting prospects. Holographic Doppler diagnostics of emerging active regions may give us insight into the prospective phenomenon of convective collapse. Holographic imaging of the tachocline, where the solar dynamo is believed to operate, may render local signatures diagnostic of future surface activity.

4.4. DEEP SOLAR INTERIOR AND FAR-SIDE SEISMIC HOLOGRAPHY

By applying the holographic regression over a large pupil we access the low- ℓ modes that penetrate deep into the solar convection zone, and which are also capable of imaging the far surface of the Sun. Considerations that apply to the computational formalism for low- ℓ holography are summarized by Section 2 of Lindsey and Braun (2000). These modes do not offer nearly as fine a spatial resolution as the high- ℓ modes used to render the images shown in this paper. However, low- ℓ phase diagnostics could shed light on some of the puzzles that have confronted models based on global diagnostics of the convection zone and the tachocline. Low- ℓ phase-sensitive holography of the far side of the Sun perhaps offers the

most promising avenues for anticipating the emergence of large active regions on the east solar limb.

4.5. MODELING AND INVERSIONS

A reliable interpretation of holographic signatures depends critically on comparisons with models to discriminate signatures of actual subsurface acoustic perturbations from artifacts, such as acoustic stalactites. Lindsey and Braun (2000) illustrate the application of simple comparative models (see Figure 5 of their paper). They briefly speculate into avenues that could lead to acoustic inversions based on holographic images.

5. Summary

The application of seismic holography to the SOHO-MDI database has given us a remarkable array of new scientific results over the past three years, opening a number of local acoustic phenomena that had hitherto been entirely undiscovered. The overall scientific results of holographic seismic imaging have generally conformed in strong agreement with those of Hankel analysis, resolving some persistent puzzles presented by the latter. What we regard as the major discoveries that have come out of seismic holography to date can be summarized as follows:

(1) *Acoustic moats surrounding sunspots*. These signatures suggest an extended, rapid outflow not far beneath the surface, probably a convection cell driven by the blockage of thermal transport by the sunspot photosphere.

(2) *Acoustic glories surrounding complex active regions*. These emit a conspicuous excess of high-frequency acoustic noise. Relative saturation of the power distribution of stochastic emission from acoustic glories may bring us some understanding of seismic emission from both the quiet Sun and the neighborhoods of active regions.

(3) *Submerged acoustic condensations* in the neighborhoods of isolated sunspots and complex active regions.

(4) *Seismic images of a large solar flare* showing a spatially extended region of acoustic emission, with high-frequency emission significantly lagging the lower frequencies.

(5) Phase-sensitive holography of active regions suggests (1) the existence of *Wilson-like depressions for all magnetic regions* approximately in logarithmic proportion to the surface magnetic pressure for $B > 10$ G, and (2) *significant sound-travel time reductions in acoustic moats*. The resulting phase shifts could explain the global frequency shifts of low-order p -modes with the solar cycle.

(6) *Anomalous acoustic reflectivity of active region subphotospheres* at high frequencies.

(7) Horizontal Doppler diagnostics indicate *rapid, extended, shallow outflows from sunspots*.

Significant prospects for seismic holography in the near future include flexible modeling of submerged thermal perturbations and flows based on holographic images, phase-correlation images of large active regions on the far side of the Sun, phase diagnostics of the deep convection zone, and certainly other possibilities that have yet to be encountered. Seismic holography is literally allowing us to look into the solar interior from a local perspective. We are only beginning to see the results of this new, powerful utility with the advent of SOHO and GONG.

Acknowledgements

We greatly appreciate the support we have gotten from the SOHO SOI-MDI team and the fine quality of the data which they have given us. We especially appreciate the conscientious support of Dr P. Scherrer, head of the SOHO-MDI project. SOHO is a project of international cooperation between ESA and NASA. D.C.B., a visitor at the Joint Institute for Laboratory Astrophysics, is grateful to Ellen Zweibel and the staff of JILA for their hospitality and support. The extraordinary dedication of our colleagues, particularly A.-C. Donea, Y. Gu, S. Jefferies, M. Fagan, Y. Fan, S. Redfield and M. Woodard have been instrumental in the successful development and fruitful application of solar acoustic holography over the past ten years. The research reviewed in this paper was supported by grants from the National Aeronautics and Space Administration and from the Solar-Terrestrial and Stellar-Astronomy-and-Astrophysics branches of the National Science Foundation.

References

- Braun, D. C.: 1995, *Astrophys. J.* **451**, 859.
 Braun, D. C.: 1997, *Astrophys. J.* **487**, 447.
 Braun, D. C. and Lindsey, C.: 1999, *Astrophys. J.* **513**, L79.
 Braun, D. C. and Lindsey, C.: 2000, *Solar Phys.* **192**, 307 (this issue).
 Braun, D. C., Duvall, T. L. Jr., and LaBonte, B. J.: 1988, *Astrophys. J.* **335**, 1015.
 Braun, D. C., Lindsey, C., Fan, Y., and Jefferies, S. M.: 1992, *Astrophys. J.* **392**, 739.
 Braun, D. C., Lindsey, C., Fan, Y., and Fagan, M.: 1998, *Astrophys. J.* **502**, 968.
 Brickhouse, N. S. and LaBonte, B. J.: 1988, *Solar Phys.* **115**, 43.
 Brown, T. M., Bogdan, T. J., Lites, B. W., and Thomas, J. H.: 1992, *Astrophys. J.* **394**, L65.
 Cally, P. S.: 2000, *Solar Phys.* **192**, 395 (this issue).
 Cally, P. S. and Bogdan, T. J.: 1997, *Astrophys. J.* **486**, L67.
 Chang, H.-K., Chou, D.-Y., LaBonte, B., and the TON Team: 1997, *Nature* **389**, 825.
 Chen, H.-R., Chou, D.-Y., Chang, H.-S., Sun, M. T., Yeh, S.-J., LaBonte, B., and the TON Team: 1998, *Astrophys. J.* **501**, L139.
 Donea, A.-C., Braun, D. C., and Lindsey, C.: 1999, *Astrophys. J.* **513**, L143.
 Donea, A.-C., Lindsey, C., and Braun, D. C.: 2000, *Solar Phys.* **192**, 321 (this issue).
 Duvall, T. L., Jr., Jefferies, S. M., Harvey, J. W., and Pomerantz, M. A.: 1993, *Nature* **362**, 430.
 Duvall T. L., Jr., D'Silva, S., Jefferies, S. M., Harvey, J. W., and Schou, J.: 1996, *Nature* **379**, 235.
 Fan, Y., Braun, D. C., and Chou D.-Y.: 1995, *Astrophys. J.* **451**, 877.

- Fox, P. A., Sofia, S. C., and Chan K. L.: 1991, *Solar Phys.* **135**, 15.
- Harvey, K. and Harvey, J.: 1973, *Solar Phys.* **28**, 61.
- Hindman, B. W. and Brown, T. M.: 1998, *Astrophys. J.* **504**, 1029.
- Jiménez-Reyes, S. J., Régulo, C., Pallé, P. L., and Roca Cortés, T.: 1998, *Astron. Astrophys.* **329**, 1119.
- Kosovichev, A. G. and Zharkova V. V.: 1998, *Nature* **393**, 317.
- Lindsey, C. and Braun, D. C.: 1990, *Solar Phys.* **126**, 101.
- Lindsey, C. and Braun, D. C.: 1997, *Astrophys. J.* **485**, 895.
- Lindsey, C. and Braun, D. C.: 1998a, *Astrophys. J.* **499**, L99.
- Lindsey, C. and Braun, D. C.: 1998b, *Astrophys. J.* **509**, L129.
- Lindsey, C. and Braun, D. C.: 1999, *Astrophys. J.* **510**, 494.
- Lindsey, C. and Braun, D. C.: 2000, *Solar Phys.* **192**, 261 (this issue).
- Lindsey, C., Braun, D. C., Jefferies, S. M., Woodard, M. F., Fan, Y., Gu, Y., and Redfield, S.: 1996, *Astrophys. J.* **470**, 636.
- Meyer, F., Schmidt, H. U., Weiss, N. O., and Wilson, P. R.: 1974, *Monthly Notices Royal Astron. Soc.* **169**, 35.
- Nye, A., Bruning, D, and LaBonte, B. J.: 1988, *Solar Phys.* **115**, 251.
- Parker, E. N.: 1974, *Solar Phys.* **36**, 249.
- Rast, M., T., Fox, P. A., Lin, H., Lites, B. W., Meisner, R. W., and White, O. R.: 1999, *Nature* **401**, 678.
- Sheeley, N. R.: 1969, *Solar Phys.* **9**, 347.